

Evidence of doubly OZI-suppressed decay $\eta_c \rightarrow \omega\phi$ in the radiative decay $J/\psi \rightarrow \gamma\eta_c$

M. Ablikim¹, M. N. Achasov^{4,c}, P. Adlarson⁷⁶, X. C. Ai⁸¹, R. Aliberti³⁵, A. Amoroso^{75A,75C}, Q. An^{72,58,a}, Y. Bai⁵⁷, O. Bakina³⁶, Y. Ban^{46,h}, H.-R. Bao⁶⁴, V. Batzskaya^{1,44}, K. Begzsuren³², N. Berger³⁵, M. Berlowski⁴⁴, M. Bertani^{28A}, D. Bettoni^{29A}, F. Bianchi^{75A,75C}, E. Bianco^{75A,75C}, A. Bortone^{75A,75C}, I. Boyko³⁶, R. A. Briere⁵, A. Brueggemann⁶⁹, H. Cai⁷⁷, M. H. Cai^{38,k,l}, X. Cai^{1,58}, A. Calcaterra^{28A}, G. F. Cao^{1,64}, N. Cao^{1,64}, S. A. Cetin^{62A}, X. Y. Chai^{46,h}, J. F. Chang^{1,58}, G. R. Che⁴³, Y. Z. Che^{1,58,64}, G. Chelkov^{36,b}, C. Chen⁴³, C. H. Chen⁹, Chao Chen⁵⁵, G. Chen¹, H. S. Chen^{1,64}, H. Y. Chen²⁰, M. L. Chen^{1,58,64}, S. J. Chen⁴², S. L. Chen⁴⁵, S. M. Chen⁶¹, T. Chen^{1,64}, X. R. Chen^{31,64}, X. T. Chen^{1,64}, Y. B. Chen^{1,58}, Y. Q. Chen³⁴, Z. J. Chen^{25,i}, Z. K. Chen⁵⁹, S. K. Choi¹⁰, X. Chu^{12,g}, G. Cibinetto^{29A}, F. Cossio^{75C}, J. J. Cui⁵⁰, H. L. Dai^{1,58}, J. P. Dai⁷⁹, A. Dbeyssi¹⁸, R. E. de Boer³, D. Dedovich³⁶, C. Q. Deng⁷³, Z. Y. Deng¹, A. Denig³⁵, I. Denysenko³⁶, M. Destefanis^{75A,75C}, F. De Mori^{75A,75C}, B. Ding^{67,1}, X. X. Ding^{46,h}, Y. Ding³⁴, Y. Ding⁴⁰, Y. X. Ding³⁰, J. Dong^{1,58}, L. Y. Dong^{1,64}, M. Y. Dong^{1,58,64}, X. Dong⁷⁷, M. C. Du¹, S. X. Du⁸¹, Y. Y. Duan⁵⁵, Z. H. Duan⁴², P. Egorov^{36,b}, G. F. Fan⁴², J. J. Fan¹⁹, Y. H. Fan⁴⁵, J. Fang⁵⁹, J. Fang^{1,58}, S. S. Fang^{1,64}, W. X. Fang¹, Y. Q. Fang^{1,58}, R. Farinelli^{29A}, L. Fava^{75B,75C}, F. Feldbauer³, G. Felici^{28A}, C. Q. Feng^{72,58}, J. H. Feng⁵⁹, Y. T. Feng^{72,58}, M. Fritsch³, C. D. Fu¹, J. L. Fu⁶⁴, Y. W. Fu^{1,64}, H. Gao⁶⁴, X. B. Gao⁴¹, Y. N. Gao^{46,h}, Y. N. Gao¹⁹, Y. Y. Gao³⁰, Yang Gao^{72,58}, S. Garbolino^{75C}, I. Garzia^{29A,29B}, P. T. Ge¹⁹, Z. W. Ge⁴², C. Geng⁵⁹, E. M. Gersabeck⁶⁸, A. Gilman⁷⁰, K. Goetzen¹³, J. D. Gong³⁴, L. Gong⁴⁰, W. X. Gong^{1,58}, W. Gradl³⁵, S. Gramigna^{29A,29B}, M. Greco^{75A,75C}, M. H. Gu^{1,58}, Y. T. Gu¹⁵, C. Y. Guan^{1,64}, A. Q. Guo³¹, L. B. Guo⁴¹, M. J. Guo⁵⁰, R. P. Guo⁴⁹, Y. P. Guo^{12,g}, A. Guskov^{36,b}, J. Gutierrez²⁷, K. L. Han⁶⁴, T. T. Han¹, F. Hanisch³, K. D. Hao^{72,58}, X. Q. Hao¹⁹, F. A. Harris⁶⁶, K. K. He⁵⁵, K. L. He^{1,64}, F. H. Heinsius³, C. H. Heinz³⁵, Y. K. Heng^{1,58,64}, C. Herold⁶⁰, T. Holtmann³, P. C. Hong³⁴, G. Y. Hou^{1,64}, X. T. Hou^{1,64}, Y. R. Hou⁶⁴, Z. L. Hou¹, B. Y. Hu⁵⁹, H. M. Hu^{1,64}, J. F. Hu^{56,j}, Q. P. Hu^{72,58}, S. L. Hu^{12,g}, T. Hu^{1,58,64}, Y. Hu¹, Z. M. Hu⁵⁹, G. S. Huang^{72,58}, K. X. Huang⁵⁹, L. Q. Huang^{31,64}, P. Huang⁴², X. T. Huang⁵⁰, Y. P. Huang¹, Y. S. Huang⁵⁹, T. Hussain⁷⁴, N. Hüsken³⁵, N. in der Wiesche⁶⁹, J. Jackson²⁷, S. Janchiv³², Q. Ji¹, Q. P. Ji¹⁹, W. Ji^{1,64}, X. B. Ji^{1,64}, X. L. Ji^{1,58}, Y. Y. Ji⁵⁰, Z. K. Jia^{72,58}, D. Jiang^{1,64}, H. B. Jiang⁷⁷, P. C. Jiang^{46,h}, S. J. Jiang⁹, T. J. Jiang¹⁶, X. S. Jiang^{1,58,64}, Y. Jiang⁶⁴, J. B. Jiao⁵⁰, J. K. Jiao³⁴, Z. Jiao²³, S. Jin⁴², Y. Jin⁶⁷, M. Q. Jing^{1,64}, X. M. Jing⁶⁴, T. Johansson⁷⁶, S. Kabana³³, N. Kalantar-Nayestanaki⁶⁵, X. L. Kang⁹, X. S. Kang⁴⁰, M. Kavatsyuk⁶⁵, B. C. Ke⁸¹, V. Khachatryan²⁷, A. Khoukaz⁶⁹, R. Kiuchi¹, O. B. Kolcu^{62A}, B. Kopf³, M. Kuessner³, X. Kui^{1,64}, N. Kumar²⁶, A. Kupsc^{44,76}, W. Kühn³⁷, Q. Lan⁷³, W. N. Lan¹⁹, T. T. Lei^{72,58}, M. Lellmann³⁵, T. Lenz³⁵, C. Li⁴³, C. Li⁴⁷, C. H. Li³⁹, C. K. Li²⁰, Cheng Li^{72,58}, D. M. Li⁸¹, F. Li^{1,58}, G. Li¹, H. B. Li^{1,64}, H. J. Li¹⁹, H. N. Li^{56,j}, Hui Li⁴³, J. R. Li⁶¹, J. S. Li⁵⁹, K. Li¹, K. L. Li^{38,k,l}, K. L. Li¹⁹, L. J. Li^{1,64}, Lei Li⁴⁸, M. H. Li⁴³, M. R. Li^{1,64}, P. L. Li⁶⁴, P. R. Li^{38,k,l}, Q. M. Li^{1,64}, Q. X. Li⁵⁰, R. Li^{17,31}, T. Li⁵⁰, T. Y. Li⁴³, W. D. Li^{1,64}, W. G. Li^{1,a}, X. Li^{1,64}, X. H. Li^{72,58}, X. L. Li⁵⁰, X. Y. Li^{1,8}, X. Z. Li⁵⁹, Y. Li¹⁹, Y. G. Li^{46,h}, Y. P. Li³⁴, Z. J. Li⁵⁹, Z. Y. Li⁷⁹, C. Liang⁴², H. Liang^{72,58}, Y. F. Liang⁵⁴, Y. T. Liang^{31,64}, G. R. Liao¹⁴, L. B. Liao⁵⁹, M. H. Liao⁵⁹, Y. P. Liao^{1,64}, J. Libby²⁶, A. Limphirat⁶⁰, C. C. Lin⁵⁵, C. X. Lin⁶⁴, D. X. Lin^{31,64}, L. Q. Lin³⁹, T. Lin¹, B. J. Liu¹, B. X. Liu⁷⁷, C. Liu³⁴, C. X. Liu¹, F. Liu¹, F. H. Liu⁵³, Feng Liu⁶, G. M. Liu^{56,j}, H. Liu^{38,k,l}, H. B. Liu¹⁵, H. H. Liu¹, H. M. Liu^{1,64}, Huihui Liu²¹, J. B. Liu^{72,58}, J. J. Liu²⁰, K. Liu^{38,k,l}, K. Liu⁷³, K. Y. Liu⁴⁰, Ke Liu²², L. Liu^{72,58}, L. C. Liu⁴³, Lu Liu⁴³, P. L. Liu¹, Q. Liu⁶⁴, S. B. Liu^{72,58}, T. Liu^{12,g}, W. K. Liu⁴³, W. M. Liu^{72,58}, W. T. Liu³⁹, X. Liu^{38,k,l}, X. Liu³⁹, X. Y. Liu⁷⁷, Y. Liu^{38,k,l}, Y. Liu⁸¹, Y. Liu⁸¹, Y. B. Liu⁴³, Z. A. Liu^{1,58,64}, Z. D. Liu⁹, Z. Q. Liu⁵⁰, X. C. Lou^{1,58,64}, F. X. Lu⁵⁹, H. J. Lu²³, J. G. Lu^{1,58}, Y. Lu⁷, Y. H. Lu^{1,64}, Y. P. Lu^{1,58}, Z. H. Lu^{1,64}, C. L. Luo⁴¹, J. R. Luo⁵⁹, J. S. Luo^{1,64}, M. X. Luo⁸⁰, T. Luo^{12,g}, X. L. Luo^{1,58}, Z. Y. Lv²², X. R. Lyu^{64,p}, Y. F. Lyu⁴³, Y. H. Lyu⁸¹, F. C. Ma⁴⁰, H. Ma⁷⁹, H. L. Ma¹, J. L. Ma^{1,64}, L. L. Ma⁵⁰, L. R. Ma⁶⁷, Q. M. Ma¹, R. Q. Ma^{1,64}, R. Y. Ma¹⁹, T. Ma^{72,58}, X. T. Ma^{1,64}, X. Y. Ma^{1,58}, Y. M. Ma³¹, F. E. Maas¹⁸, I. MacKay⁷⁰, M. Maggiora^{75A,75C}, S. Malde⁷⁰, Y. J. Mao^{46,h}, Z. P. Mao¹, S. Marcello^{75A,75C}, F. M. Melendi^{29A,29B}, Y. H. Meng⁶⁴, Z. X. Meng⁶⁷, J. G. Messchendorp^{13,65}, G. Mezzadri^{29A}, H. Miao^{1,64}, T. J. Min⁴², R. E. Mitchell²⁷, X. H. Mo^{1,58,64}, B. Moses²⁷, N. Yu. Muchnoi^{4,c}, J. Muskalla³⁵, Y. Nefedov³⁶, F. Nerling^{18,e}, L. S. Nie²⁰, I. B. Nikolaev^{4,c}, Z. Ning^{1,58}, S. Nisar^{11,m}, Q. L. Niu^{38,k,l}, W. D. Niu^{12,g}, S. L. Olsen^{10,64}, Q. Ouyang^{1,58,64}, S. Pacetti^{28B,28C}, X. Pan⁵⁵, Y. Pan⁵⁷, A. Pathak¹⁰, Y. P. Pei^{72,58}, M. Pelizaeus³, H. P. Peng^{72,58}, Y. Y. Peng^{38,k,l}, K. Peters^{13,e}, J. L. Ping⁴¹, R. G. Ping^{1,64}, S. Plura³⁵, V. Prasad³³, F. Z. Qi¹, H. R. Qi⁶¹, M. Qi⁴², S. Qian^{1,58}, W. B. Qian⁶⁴, C. F. Qiao⁶⁴, J. H. Qiao¹⁹, J. J. Qin⁷³, J. L. Qin⁵⁵, L. Q. Qin¹⁴, L. Y. Qin^{72,58}, P. B. Qin⁷³, X. P. Qin^{12,g}, X. S. Qin⁵⁰, Z. H. Qin^{1,58}, J. F. Qiu¹, Z. H. Qu⁷³, C. F. Redmer³⁵, A. Rivetti^{75C}, M. Rolo^{75C}, G. Rong^{1,64}, S. S. Rong^{1,64}, F. Rosini^{28B,28C}, Ch. Rosner¹⁸, M. Q. Ruan^{1,58}, S. N. Ruan⁴³, N. Salone⁴⁴, A. Sarantsev^{36,d}, Y. Schelhaas³⁵, K. Schoenning⁷⁶, M. Scodreggio^{29A}, K. Y. Shan^{12,g}, W. Shan²⁴, X. Y. Shan^{72,58}, Z. J. Shang^{38,k,l}, J. F. Shangguan¹⁶, L. G. Shao^{1,64}, M. Shao^{72,58}, C. P. Shen^{12,g}, H. F. Shen^{1,8}, W. H. Shen⁶⁴, X. Y. Shen^{1,64}, B. A. Shi⁶⁴, H. Shi^{72,58}, J. L. Shi^{12,g}, J. Y. Shi¹, S. Y. Shi⁷³, X. Shi^{1,58}, H. L. Song^{72,58}, J. J. Song¹⁹, T. Z. Song⁵⁹, W. M. Song^{34,1}, Y. X. Song^{46,h,n}, S. Sosio^{75A,75C}, S. Spataro^{75A,75C}, F. Stieler³⁵, S. S. Su⁴⁰, Y. J. Su⁶⁴, G. B. Sun⁷⁷, G. X. Sun¹, H. Sun⁶⁴, H. K. Sun¹, J. F. Sun¹⁹, K. Sun⁶¹, L. Sun⁷⁷, S. S. Sun^{1,64}, T. Sun^{51,f}, Y. C. Sun⁷⁷, Y. H. Sun³⁰, Y. J. Sun^{72,58}, Y. Z. Sun¹, Z. Q. Sun^{1,64},

Z. T. Sun⁵⁰, C. J. Tang⁵⁴, G. Y. Tang¹, J. Tang⁵⁹, L. F. Tang³⁹, M. Tang^{72,58}, Y. A. Tang⁷⁷, L. Y. Tao⁷³, M. Tat⁷⁰, J. X. Teng^{72,58}, J. Y. Tian^{72,58}, W. H. Tian⁵⁹, Y. Tian³¹, Z. F. Tian⁷⁷, I. Uman^{62B}, B. Wang⁵⁹, B. Wang¹, Bo Wang^{72,58}, C. Wang¹⁹, Cong Wang²², D. Y. Wang^{46,h}, H. J. Wang^{38,k,l}, J. J. Wang⁷⁷, K. Wang^{1,58}, L. L. Wang¹, L. W. Wang³⁴, M. Wang⁵⁰, M. Wang^{72,58}, N. Y. Wang⁶⁴, S. Wang^{12,g}, T. Wang^{12,g}, T. J. Wang⁴³, W. Wang⁷³, W. Wang⁵⁹, W. P. Wang^{35,58,72,o}, X. Wang^{46,h}, X. F. Wang^{38,k,l}, X. J. Wang³⁹, X. L. Wang^{12,g}, X. N. Wang¹, Y. Wang⁶¹, Y. D. Wang⁴⁵, Y. F. Wang^{1,58,64}, Y. H. Wang^{38,k,l}, Y. L. Wang¹⁹, Y. N. Wang⁷⁷, Y. Q. Wang¹, Yaqian Wang¹⁷, Yi Wang⁶¹, Yuan Wang^{17,31}, Z. Wang^{1,58}, Z. L. Wang⁷³, Z. L. Wang², Z. Q. Wang^{12,g}, Z. Y. Wang^{1,64}, D. H. Wei¹⁴, H. R. Wei⁴³, F. Weidner⁶⁹, S. P. Wen¹, Y. R. Wen³⁹, U. Wiedner³, G. Wilkinson⁷⁰, M. Wolke⁷⁶, C. Wu³⁹, J. F. Wu^{1,8}, L. H. Wu¹, L. J. Wu^{1,64}, Lianjie Wu¹⁹, S. G. Wu^{1,64}, S. M. Wu⁶⁴, X. Wu^{12,g}, X. H. Wu³⁴, Y. J. Wu³¹, Z. Wu^{1,58}, L. Xia^{72,58}, X. M. Xian³⁹, B. H. Xiang^{1,64}, T. Xiang^{46,h}, D. Xiao^{38,k,l}, G. Y. Xiao⁴², H. Xiao⁷³, Y. L. Xiao^{12,g}, Z. J. Xiao⁴¹, C. Xie⁴², K. J. Xie^{1,64}, X. H. Xie^{46,h}, Y. Xie⁵⁰, Y. G. Xie^{1,58}, Y. H. Xie⁶, Z. P. Xie^{72,58}, T. Y. Xing^{1,64}, C. F. Xu^{1,64}, C. J. Xu⁵⁹, G. F. Xu¹, H. Y. Xu², H. Y. Xu^{67,2}, M. Xu^{72,58}, Q. J. Xu¹⁶, Q. N. Xu³⁰, W. L. Xu⁶⁷, X. P. Xu⁵⁵, Y. Xu⁴⁰, Y. Xu^{12,g}, Y. C. Xu⁷⁸, Z. S. Xu⁶⁴, H. Y. Yan³⁹, L. Yan^{12,g}, W. B. Yan^{72,58}, W. C. Yan⁸¹, W. P. Yan¹⁹, X. Q. Yan^{1,64}, H. J. Yang^{51,f}, H. L. Yang³⁴, H. X. Yang¹, J. H. Yang⁴², R. J. Yang¹⁹, T. Yang¹, Y. Yang^{12,g}, Y. F. Yang⁴³, Y. H. Yang⁴², Y. Q. Yang⁹, Y. X. Yang^{1,64}, Y. Z. Yang¹⁹, M. Ye^{1,58}, M. H. Ye⁸, Junhao Yin⁴³, Z. Y. You⁵⁹, B. X. Yu^{1,58,64}, C. X. Yu⁴³, G. Yu¹³, J. S. Yu^{25,i}, M. C. Yu⁴⁰, T. Yu⁷³, X. D. Yu^{46,h}, Y. C. Yu⁸¹, C. Z. Yuan^{1,64}, H. Yuan^{1,64}, J. Yuan⁴⁵, J. Yuan³⁴, L. Yuan², S. C. Yuan^{1,64}, Y. Yuan^{1,64}, Z. Y. Yuan⁵⁹, C. X. Yue³⁹, Ying Yue¹⁹, A. A. Zafar⁷⁴, S. H. Zeng^{63A,63B,63C,63D}, X. Zeng^{12,g}, Y. Zeng^{25,i}, Y. J. Zeng^{1,64}, Y. J. Zeng⁵⁹, X. Y. Zhai³⁴, Y. H. Zhan⁵⁹, A. Q. Zhang^{1,64}, B. L. Zhang^{1,64}, B. X. Zhang¹, D. H. Zhang⁴³, G. Y. Zhang¹⁹, G. Y. Zhang^{1,64}, H. Zhang^{72,58}, H. Zhang⁸¹, H. C. Zhang^{1,58,64}, H. H. Zhang⁵⁹, H. Q. Zhang^{1,58,64}, H. R. Zhang^{72,58}, H. Y. Zhang^{1,58}, J. Zhang⁵⁹, J. Zhang⁸¹, J. J. Zhang⁵², J. L. Zhang²⁰, J. Q. Zhang⁴¹, J. S. Zhang^{12,g}, J. W. Zhang^{1,58,64}, J. X. Zhang^{38,k,l}, J. Y. Zhang¹, J. Z. Zhang^{1,64}, Jianyu Zhang⁶⁴, L. M. Zhang⁶¹, Lei Zhang⁴², N. Zhang⁸¹, P. Zhang^{1,64}, Q. Zhang¹⁹, Q. Y. Zhang³⁴, R. Y. Zhang^{38,k,l}, S. H. Zhang^{1,64}, Shulei Zhang^{25,i}, X. M. Zhang¹, X. Y. Zhang⁴⁰, X. Y. Zhang⁵⁰, Y. Zhang⁷³, Y. Zhang¹, Y. T. Zhang⁸¹, Y. H. Zhang^{1,58}, Y. M. Zhang³⁹, Z. D. Zhang¹, Z. H. Zhang¹, Z. L. Zhang³⁴, Z. L. Zhang⁵⁵, Z. X. Zhang¹⁹, Z. Y. Zhang⁴³, Z. Y. Zhang⁷⁷, Z. Z. Zhang⁴⁵, Zh. Zh. Zhang¹⁹, G. Zhao¹, J. Y. Zhao^{1,64}, J. Z. Zhao^{1,58}, L. Zhao¹, Lei Zhao^{72,58}, M. G. Zhao⁴³, N. Zhao⁷⁹, R. P. Zhao⁶⁴, S. J. Zhao⁸¹, Y. B. Zhao^{1,58}, Y. L. Zhao⁵⁵, Y. X. Zhao^{31,64}, Z. G. Zhao^{72,58}, A. Zhemchugov^{36,b}, B. Zheng⁷³, B. M. Zheng³⁴, J. P. Zheng^{1,58}, W. J. Zheng^{1,64}, X. R. Zheng¹⁹, Y. H. Zheng^{64,p}, B. Zhong⁴¹, X. Zhong⁵⁹, H. Zhou^{35,50,o}, J. Q. Zhou³⁴, J. Y. Zhou³⁴, S. Zhou⁶, X. Zhou⁷⁷, X. K. Zhou⁶, X. R. Zhou^{72,58}, X. Y. Zhou³⁹, Y. Z. Zhou^{12,g}, Z. C. Zhou²⁰, A. N. Zhu⁶⁴, J. Zhu⁴³, K. Zhu¹, K. J. Zhu^{1,58,64}, K. S. Zhu^{12,g}, L. Zhu³⁴, L. X. Zhu⁶⁴, S. H. Zhu⁷¹, T. J. Zhu^{12,g}, W. D. Zhu^{12,g}, W. D. Zhu⁴¹, W. J. Zhu¹, W. Z. Zhu¹⁹, Y. C. Zhu^{72,58}, Z. A. Zhu^{1,64}, X. Y. Zhuang⁴³, J. H. Zou¹, J. Zu^{72,58}

(BESIII Collaboration)

¹ *Institute of High Energy Physics, Beijing 100049, People's Republic of China*

² *Beihang University, Beijing 100191, People's Republic of China*

³ *Bochum Ruhr-University, D-44780 Bochum, Germany*

⁴ *Budker Institute of Nuclear Physics SB RAS (BINP), Novosibirsk 630090, Russia*

⁵ *Carnegie Mellon University, Pittsburgh, Pennsylvania 15213, USA*

⁶ *Central China Normal University, Wuhan 430079, People's Republic of China*

⁷ *Central South University, Changsha 410083, People's Republic of China*

⁸ *China Center of Advanced Science and Technology, Beijing 100190, People's Republic of China*

⁹ *China University of Geosciences, Wuhan 430074, People's Republic of China*

¹⁰ *Chung-Ang University, Seoul, 06974, Republic of Korea*

¹¹ *COMSATS University Islamabad, Lahore Campus, Defence Road, Off Raiwind Road, 54000 Lahore, Pakistan*

¹² *Fudan University, Shanghai 200433, People's Republic of China*

¹³ *GSI Helmholtzcentre for Heavy Ion Research GmbH, D-64291 Darmstadt, Germany*

¹⁴ *Guangxi Normal University, Guilin 541004, People's Republic of China*

¹⁵ *Guangxi University, Nanning 530004, People's Republic of China*

¹⁶ *Hangzhou Normal University, Hangzhou 310036, People's Republic of China*

¹⁷ *Hebei University, Baoding 071002, People's Republic of China*

¹⁸ *Helmholtz Institute Mainz, Staudinger Weg 18, D-55099 Mainz, Germany*

¹⁹ *Henan Normal University, Xinxiang 453007, People's Republic of China*

²⁰ *Henan University, Kaifeng 475004, People's Republic of China*

²¹ *Henan University of Science and Technology, Luoyang 471003, People's Republic of China*

²² *Henan University of Technology, Zhengzhou 450001, People's Republic of China*

²³ *Huangshan College, Huangshan 245000, People's Republic of China*

- ²⁴ Hunan Normal University, Changsha 410081, People's Republic of China
- ²⁵ Hunan University, Changsha 410082, People's Republic of China
- ²⁶ Indian Institute of Technology Madras, Chennai 600036, India
- ²⁷ Indiana University, Bloomington, Indiana 47405, USA
- ²⁸ INFN Laboratori Nazionali di Frascati, (A)INFN Laboratori Nazionali di Frascati, I-00044, Frascati, Italy; (B)INFN Sezione di Perugia, I-06100, Perugia, Italy; (C)University of Perugia, I-06100, Perugia, Italy
- ²⁹ INFN Sezione di Ferrara, (A)INFN Sezione di Ferrara, I-44122, Ferrara, Italy; (B)University of Ferrara, I-44122, Ferrara, Italy
- ³⁰ Inner Mongolia University, Hohhot 010021, People's Republic of China
- ³¹ Institute of Modern Physics, Lanzhou 730000, People's Republic of China
- ³² Institute of Physics and Technology, Peace Avenue 54B, Ulaanbaatar 13330, Mongolia
- ³³ Instituto de Alta Investigación, Universidad de Tarapacá, Casilla 7D, Arica 1000000, Chile
- ³⁴ Jilin University, Changchun 130012, People's Republic of China
- ³⁵ Johannes Gutenberg University of Mainz, Johann-Joachim-Becher-Weg 45, D-55099 Mainz, Germany
- ³⁶ Joint Institute for Nuclear Research, 141980 Dubna, Moscow region, Russia
- ³⁷ Justus-Liebig-Universität Giessen, II. Physikalisches Institut, Heinrich-Buff-Ring 16, D-35392 Giessen, Germany
- ³⁸ Lanzhou University, Lanzhou 730000, People's Republic of China
- ³⁹ Liaoning Normal University, Dalian 116029, People's Republic of China
- ⁴⁰ Liaoning University, Shenyang 110036, People's Republic of China
- ⁴¹ Nanjing Normal University, Nanjing 210023, People's Republic of China
- ⁴² Nanjing University, Nanjing 210093, People's Republic of China
- ⁴³ Nankai University, Tianjin 300071, People's Republic of China
- ⁴⁴ National Centre for Nuclear Research, Warsaw 02-093, Poland
- ⁴⁵ North China Electric Power University, Beijing 102206, People's Republic of China
- ⁴⁶ Peking University, Beijing 100871, People's Republic of China
- ⁴⁷ Qufu Normal University, Qufu 273165, People's Republic of China
- ⁴⁸ Renmin University of China, Beijing 100872, People's Republic of China
- ⁴⁹ Shandong Normal University, Jinan 250014, People's Republic of China
- ⁵⁰ Shandong University, Jinan 250100, People's Republic of China
- ⁵¹ Shanghai Jiao Tong University, Shanghai 200240, People's Republic of China
- ⁵² Shanxi Normal University, Linfen 041004, People's Republic of China
- ⁵³ Shanxi University, Taiyuan 030006, People's Republic of China
- ⁵⁴ Sichuan University, Chengdu 610064, People's Republic of China
- ⁵⁵ Soochow University, Suzhou 215006, People's Republic of China
- ⁵⁶ South China Normal University, Guangzhou 510006, People's Republic of China
- ⁵⁷ Southeast University, Nanjing 211100, People's Republic of China
- ⁵⁸ State Key Laboratory of Particle Detection and Electronics, Beijing 100049, Hefei 230026, People's Republic of China
- ⁵⁹ Sun Yat-Sen University, Guangzhou 510275, People's Republic of China
- ⁶⁰ Suranaree University of Technology, University Avenue 111, Nakhon Ratchasima 30000, Thailand
- ⁶¹ Tsinghua University, Beijing 100084, People's Republic of China
- ⁶² Turkish Accelerator Center Particle Factory Group, (A)Istinye University, 34010, Istanbul, Turkey; (B)Near East University, Nicosia, North Cyprus, 99138, Mersin 10, Turkey
- ⁶³ University of Bristol, H H Wills Physics Laboratory, Tyndall Avenue, Bristol, BS8 1TL, UK
- ⁶⁴ University of Chinese Academy of Sciences, Beijing 100049, People's Republic of China
- ⁶⁵ University of Groningen, NL-9747 AA Groningen, The Netherlands
- ⁶⁶ University of Hawaii, Honolulu, Hawaii 96822, USA
- ⁶⁷ University of Jinan, Jinan 250022, People's Republic of China
- ⁶⁸ University of Manchester, Oxford Road, Manchester, M13 9PL, United Kingdom
- ⁶⁹ University of Muenster, Wilhelm-Klemm-Strasse 9, 48149 Muenster, Germany
- ⁷⁰ University of Oxford, Keble Road, Oxford OX13RH, United Kingdom
- ⁷¹ University of Science and Technology Liaoning, Anshan 114051, People's Republic of China
- ⁷² University of Science and Technology of China, Hefei 230026, People's Republic of China
- ⁷³ University of South China, Hengyang 421001, People's Republic of China
- ⁷⁴ University of the Punjab, Lahore-54590, Pakistan
- ⁷⁵ University of Turin and INFN, (A)University of Turin, I-10125, Turin, Italy; (B)University of Eastern Piedmont, I-15121, Alessandria, Italy; (C)INFN, I-10125, Turin, Italy

⁷⁶ Uppsala University, Box 516, SE-75120 Uppsala, Sweden

⁷⁷ Wuhan University, Wuhan 430072, People's Republic of China

⁷⁸ Yantai University, Yantai 264005, People's Republic of China

⁷⁹ Yunnan University, Kunming 650500, People's Republic of China

⁸⁰ Zhejiang University, Hangzhou 310027, People's Republic of China

⁸¹ Zhengzhou University, Zhengzhou 450001, People's Republic of China

^a Deceased

^b Also at the Moscow Institute of Physics and Technology, Moscow 141700, Russia

^c Also at the Novosibirsk State University, Novosibirsk, 630090, Russia

^d Also at the NRC "Kurchatov Institute", PNPI, 188300, Gatchina, Russia

^e Also at Goethe University Frankfurt, 60323 Frankfurt am Main, Germany

^f Also at Key Laboratory for Particle Physics, Astrophysics and Cosmology, Ministry of Education; Shanghai Key Laboratory for Particle Physics and Cosmology; Institute of Nuclear and Particle Physics, Shanghai 200240, People's Republic of China

^g Also at Key Laboratory of Nuclear Physics and Ion-beam Application (MOE) and Institute of Modern Physics, Fudan University, Shanghai 200443, People's Republic of China

^h Also at State Key Laboratory of Nuclear Physics and Technology, Peking University, Beijing 100871, People's Republic of China

ⁱ Also at School of Physics and Electronics, Hunan University, Changsha 410082, China

^j Also at Guangdong Provincial Key Laboratory of Nuclear Science, Institute of Quantum Matter, South China Normal University, Guangzhou 510006, China

^k Also at MOE Frontiers Science Center for Rare Isotopes, Lanzhou University, Lanzhou 730000, People's Republic of China

^l Also at Lanzhou Center for Theoretical Physics, Lanzhou University, Lanzhou 730000, People's Republic of China

^m Also at the Department of Mathematical Sciences, IBA, Karachi 75270, Pakistan

ⁿ Also at Ecole Polytechnique Federale de Lausanne (EPFL), CH-1015 Lausanne, Switzerland

^o Also at Helmholtz Institute Mainz, Staudinger Weg 18, D-55099 Mainz, Germany

^p Also at Hangzhou Institute for Advanced Study, University of Chinese Academy of Sciences, Hangzhou 310024, China

(Dated: April 3, 2025)

Using a sample of $(10087 \pm 44) \times 10^6$ J/ψ events collected with the BESIII detector at the BEPCII collider, the first evidence for the doubly OZI-suppressed decay $\eta_{c\text{as}d\text{as}d} \rightarrow \omega\phi$ is reported with a significance of 4.0σ . The branching fraction of $\eta_c \rightarrow \omega\phi$ is measured to be $\mathcal{B}(\eta_c \rightarrow \omega\phi) = (3.86 \pm 0.92 \pm 0.62) \times 10^{-5}$, where the first uncertainty is statistical and the second is systematic. This result provides valuable insights into the underlying mechanisms of charmonium decays, particularly for processes such as $\eta_c \rightarrow VV$ (where V represents a vector meson).

I. INTRODUCTION

The η_c , as the lightest and S -wave spin-singlet charmonium state, plays a fundamental role in the study of charmonium decays. Although η_c was observed by the Crystal Ball experiment [1] more than forty years ago, its properties remain under investigation. To date, only the exclusive decay modes with a total branching fraction of approximately 60% have been experimentally observed, many of which are measured with limited precision and large uncertainties [2]. As a result, our understanding of the η_c properties remains incomplete.

The decays of η_c into vector meson pairs ($\eta_c \rightarrow VV$, where V denotes a vector meson), which are Okubo-Zweig-Iizuka (OZI) suppressed processes [3], have long posed a significant puzzle in charmonium physics. According to the Helicity Selection Rule (HSR) [4], these decays are highly suppressed at leading order in Quantum Chromodynamics (QCD). The branching fractions of $\eta_c \rightarrow \omega\omega$ and $\eta_c \rightarrow \phi\phi$ have been well measured by the Beijing Spectrometer III (BESIII) experiment [5, 6] and

Belle experiment [7]. However, both results are significantly larger than theoretical predictions [8], challenging explanations based solely on the quark model and perturbative QCD calculations. Non-perturbative models, such as the intermediate meson exchange model [9] and the charmonium light Fock component admixture model [10], have been proposed as potential solutions. Nevertheless, further investigations are required to fully understand these processes.

The decay $\eta_c \rightarrow \omega\phi$, which proceeds via a doubly OZI (DOZI) suppressed process as shown by the Feynman diagram in Fig. 1, is expected to provide deeper insights into the underlying mechanisms of decays $\eta_c \rightarrow VV$. Such insights could offer valuable constraints for theoretical models. Several well-established models have been developed to study the mechanisms of DOZI decays in J/ψ and η_c systems [11, 12]. However, among the DOZI decays of η_c , the decay $\eta_c \rightarrow \omega\phi$ has neither been observed experimentally nor investigated theoretically. To date, only an upper limit on its branching fraction has been reported by BESIII, based on a sample of $(223.7 \pm 1.4) \times 10^6$ J/ψ

events [6].

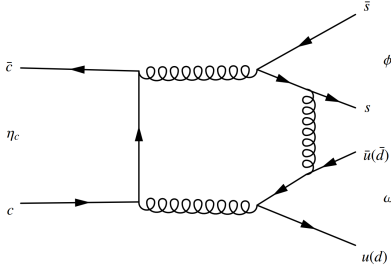


FIG. 1. An example of Feynman diagram for $\eta_c \rightarrow \omega\phi$.

In this paper, utilizing a significantly larger data sample of $(10087 \pm 44) \times 10^6$ J/ψ events [13] accumulated at the BESIII detector, we present the first evidence for $\eta_c \rightarrow \omega\phi$ and determine its branching fraction, benefiting from both the increased data sample and an improved method for background suppression.

II. BESIII DETECTOR AND MONTE CARLO SIMULATION

The BESIII detector [14] records symmetric e^+e^- collision events provided by the BEPCII storage ring [15] in the center-of-mass energy ranging from 1.84 to 4.95 GeV, with an achieved peak luminosity of $1.1 \times 10^{33} \text{ cm}^{-2}\text{s}^{-1}$ at $\sqrt{s} = 3.773 \text{ GeV}$. BESIII has collected large data samples in this energy region [16]. The cylindrical core of the BESIII detector covers 93% of the full solid angle and consists of a helium-based multilayer drift chamber (MDC), a plastic scintillator time-of-flight system (TOF), and a CsI(Tl) electromagnetic calorimeter (EMC), which are all enclosed in a superconducting solenoidal magnet providing a 1.0 T magnetic field. The magnetic field was 0.9 T in 2012, which affects 11% of the total J/ψ data. The solenoid is supported by an octagonal flux-return yoke with resistive plate counter muon identification modules interleaved with steel. The momentum resolution of charged particle at 1 GeV/c is 0.5%, and the dE/dx resolution is 6% for electrons from Bhabha scattering. The EMC measures photon energies with a resolution of 2.5% (5%) at 1 GeV in the barrel (end cap) region. The time resolution in the TOF barrel region is 68 ps, while that in the end cap region was 110 ps. The end cap TOF system was upgraded in 2015 using multigap resistive plate chamber technology, provides a time resolution of 60 ps, which benefits 87% of the data used in this analysis [17–19].

Simulated data samples produced with a GEANT4-based [20] Monte Carlo (MC) package, which includes the geometric description of the BESIII detector and the detector response, are used to optimize the selection criteria, to determine the detection efficiencies and to estimate backgrounds. In the simulation, the beam energy spread and initial state radiation in the e^+e^- annihilations are modeled with the generator KKMC [21]. An inclusive MC sample consisted of 10^{10} J/ψ events, including the pro-

duction of the J/ψ resonance, are generated to study the backgrounds. All particle decays are modelled either with EVTGEN [22, 23] using branching fractions taken from the Particle Data Group (PDG) [2], when available, or otherwise estimated with LUNDCHARM [24, 25] package. Final state radiation from charged final state particles is incorporated using the PHOTOS package [26]. The signal events from $J/\psi \rightarrow \gamma\eta_c$ are generated with the modified JPE model [27, 28]. In this model, the M1 transition is assumed to follow the form factor $E_\gamma^3 \times \exp(-E_\gamma^2/8\beta^2)$ with $\beta = 65.0 \pm 2.5 \text{ MeV}$. Here, E_γ represents the energy of the radiative photon. These parameters also follow the previous results [27] with the η_c mass $2984.1 \text{ MeV}/c^2$ and the width 30.5 MeV. The decays $\eta_c \rightarrow \omega\phi$, $\omega \rightarrow \pi^+\pi^-\pi^0$, $\pi^0 \rightarrow \gamma\gamma$ and $\phi \rightarrow K^+K^-$ are generated with the EVTGEN generator [22, 23] model. Specifically, the $\eta_c \rightarrow \omega\phi$ decay is generated with HELAMP model; the $\omega \rightarrow \pi^+\pi^-\pi^0$ decay is generated by the OMEGA DALITZ model [29]; and the $\phi \rightarrow K^+K^-$ decay is generated by the VSS model.

III. EVENT SELECTION

A. Common selection

In this analysis, the η_c candidates are produced via the radiative decay $J/\psi \rightarrow \gamma\eta_c$. Consequently, the $\eta_c \rightarrow \omega\phi$ candidates are selected via the final state of $3\gamma\pi^+\pi^-K^+K^-$. Candidate events are required to have exactly four charged tracks with zero net charge and at least three photon candidates.

Charged tracks detected in the MDC are required to satisfy $|\cos\theta| < 0.93$, where θ is the polar angle defined with respect to the z -axis of the BESIII detector. The distance of closest approach to the interaction point (IP) must be less than 10 cm along the z -axis, and less than 1 cm in the transverse plane. Particle identification (PID) for charged tracks combines the specific ionization energy loss (dE/dx) measured by the MDC and the flight time in the TOF to form the likelihood values $\mathcal{L}(h)$ for $h = K$ and π hypotheses, individually. Charged kaons and pions are identified by requiring $\mathcal{L}(K) > \mathcal{L}(\pi)$ and $\mathcal{L}(\pi) > \mathcal{L}(K)$, respectively.

Photon candidates are identified using isolated showers in the EMC. The deposited energy of each shower must be more than 25 MeV in the barrel region ($|\cos\theta| < 0.80$) or more than 50 MeV in the end cap region ($0.86 < |\cos\theta| < 0.92$). To exclude showers originating from charged tracks, the opening angle subtended by the EMC shower and the position of the closest charged track at the EMC must be greater than 10 degrees as measured from the IP. To suppress electronic noise and showers unrelated to the event, the difference between the EMC time and the event start time is required to be within [0, 700] ns.

A primary vertex fit is performed for the selected $K^+K^-\pi^+\pi^-$ candidate, and a successful vertex fit is required. To improve the resolution and suppress background contributions, a five-constraint (5C) kinematic fit is performed by imposing energy-momentum conservation under the hypothesis of $K^+K^-\pi^+\pi^-\gamma\gamma\gamma$, with the in-

variant mass of two photons constrained to the known π^0 mass [2]. The best combination is selected based on the minimum χ_{5C}^2 , and events are required to satisfy $\chi_{5C}^2 < 20$ for further analysis. This requirement is determined by optimizing the Figure-of-Merit $S/\sqrt{S+B}$, where S is the number of signal events from the signal MC sample and $S+B$ is the total number of events in data.

B. Further selection

Additional selection criteria are applied to further suppress the significant background contributions. To suppress the background from events without π^0 in the final state and to minimize the wrong combination of π^0 for the signal, the decay angle of π^0 is defined as

$$\cos(\theta_{\text{decay}}) = \frac{E_{\gamma_1} - E_{\gamma_2}}{p_{\gamma_1\gamma_2}}, \quad (1)$$

where γ_1 and γ_2 are the photons forming the π^0 , E_{γ_1} and E_{γ_2} are the energies of photons, and $p_{\gamma_1\gamma_2}$ is the momentum of the two-photon system. A requirement of $|\cos(\theta_{\text{decay}})| < 0.95$ is imposed. Studies based on the signal MC sample indicate that this π^0 decay angle requirement reduces the wrong combination rate of π^0 candidates to less than 1%.

After applying all the above selection criteria, the distribution of the invariant masses of $\pi^+\pi^-\pi^0$ and K^+K^- , $M_{\pi^+\pi^-\pi^0}$ versus $M_{K^+K^-}$ for the accepted candidates in data, is shown in Fig. 2. In this figure, a cluster of events is observed in the $\omega\phi$ signal region, along with a horizontal band for the ϕ signal and a vertical band for the ω signal. The $\omega\phi$ signal region is defined as $|M_{\pi^+\pi^-\pi^0} - M_{\omega}^{\text{PDG}}| < 40.0 \text{ MeV}/c^2$, and $|M_{K^+K^-} - M_{\phi}^{\text{PDG}}| < 15.0 \text{ MeV}/c^2$, as shown in Fig. 2. These signal regions are set to be approximately three times the fitted mass resolution around the known ω and ϕ masses [2]. To further suppress backgrounds from processes such as $J/\psi \rightarrow \phi\eta'$, $\eta' \rightarrow \gamma\omega$, $\omega \rightarrow \pi^+\pi^-\pi^0$, $\pi^0 \rightarrow \gamma\gamma$, an η' veto is applied. Events with an invariant mass $M_{\pi^+\pi^-\pi^0}$ in the range $943.0 < M_{\pi^+\pi^-\pi^0} < 969.0 \text{ MeV}/c^2$ are vetoed.

After applying all the event selection criteria, the distribution of the invariant mass $M_{K^+K^-\pi^+\pi^-\pi^0}$ for the surviving candidate events in data is shown in Fig. 3. In this figure, the η_c signal is clearly observed. A prominent J/ψ peak is also visible, indicating the presence of background events with a $K^+K^-\pi^+\pi^-\pi^0$ final state but without a radiative photon. A more detailed discussion of this figure is provided in the second paragraph of Sec. IV.

IV. BACKGROUND SUBTRACTION

A. Background study

The potential background contributions are investigated based on the analysis of J/ψ inclusive MC sample with a topology analysis tool [30]. The background is found to be relatively high and can be categorized into two types,

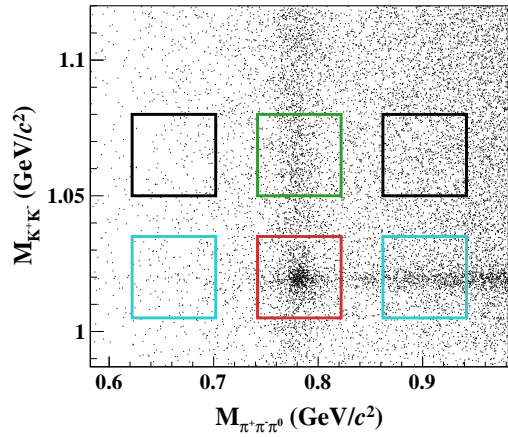


FIG. 2. The distribution of $M_{\pi^+\pi^-\pi^0}$ versus $M_{K^+K^-}$. The horizontal and vertical bands correspond to the ϕ and ω signal regions, respectively. The red box represents the $\omega\phi$ signal region. The green box represents the ϕ sideband region (right ω and wrong ϕ). The cyan boxes represent the ω sideband region (wrong ω and right ϕ). The black boxes represent the non- ω/ϕ region (wrong ω and wrong ϕ). Because of the phase-space limitation there are not enough events below $0.9 \text{ GeV}/c^2$ in $M_{K^+K^-}$.

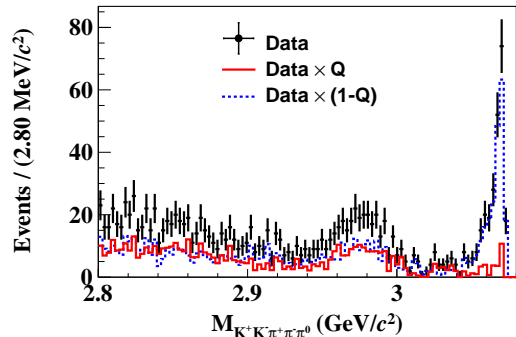


FIG. 3. The distribution of $M_{K^+K^-\pi^+\pi^-\pi^0}$ for the survived candidate events in the $\omega\phi$ signal region. The black dots represent data, the red line is for the Q-weighted events and the blue dotted line is for the $(1-Q)$ -weighted events. These notations Q and $1-Q$ represent the probabilities by which an event is defined to be signal and background, respectively (further details will be in the next section).

i.e. background without ω or ϕ (namely non- ω/ϕ background thereafter) and background with $\omega\phi$ but no η_c intermediate state (namely non- η_c background). Due to possible decays such as $\eta_c \rightarrow \omega K^+K^-$, $\eta_c \rightarrow \phi\pi^+\pi^-\pi^0$ and $\eta_c \rightarrow K^+K^-\pi^+\pi^-\pi^0$ (without intermediate states), these backgrounds may produce a peak in the η_c region of the $M_{K^+K^-\pi^+\pi^-\pi^0}$ distribution. Because of the C-parity conservation, backgrounds from $J/\psi \rightarrow \omega\phi$ and $J/\psi \rightarrow \pi^0\omega\phi$ are forbidden.

B. Non- $\omega\phi$ background estimation

To estimate the contribution of the non- ω/ϕ background, a Q-weight method is employed. This method, detailed in Ref. [31], assigns a weight to each event, representing its probability of being signal or background. The Q-weight method has been widely used in experiments such as CLAS, Crystal Barrel and BESIII [5, 32, 33]. The sum of the Q-weights for all events corresponds to the number of signal events, while the sum of (1 - Q)-weights corresponds to the number of background events. In the Q-weight method, a set of phase space (PHSP) variables $\vec{\xi}$ is used to select a control sample for each event. The PHSP distance $d_{i,j}^2$ between the i -th and j -th events is defined as:

$d_{i,j}^2 = \sum_k \left(\frac{\xi_k^i - \xi_k^j}{\Delta_k} \right)^2$, where Δ_k is a normalization factor for the k -th variable. For each event, a control sample of 200 events with the smallest $d_{i,j}^2$ is selected.

Based on the selected control sample, a fit on the distribution of a set of discrimination variables \vec{v} is carried out to extract the yields of signal and background, and the signal weight for the i -th event is obtained with the ratio of signal yield from the fit to the number of control sample. The PHSP variables $\vec{\xi}$ and the corresponding normalization factors Δ_k are listed in Table I. For events with $M_{K^+K^-\pi^+\pi^-\pi^0} < 2950.0$ MeV/ c^2 , all PHSP variables are used. For events with $M_{K^+K^-\pi^+\pi^-\pi^0} \geq 2950.0$ MeV/ c^2 , only the $m^2(\omega\phi)$ is used due to significant changes in its distribution. The control sample is selected from candidate events within a broad range of $M_{K^+K^-}$ and $M_{\pi^+\pi^-\pi^0}$: $M_{K^+K^-} < 1120.0$ MeV/ c^2 and $582.0 < M_{\pi^+\pi^-\pi^0} < 982.0$ MeV/ c^2 (see Fig. 2). The variables $M_{K^+K^-}$ and $M_{\pi^+\pi^-\pi^0}$ are used as discrimination variables \vec{v} . A two-dimensional (2-D) unbinned maximum likelihood fit is performed on the distribution of $M_{K^+K^-}$ versus $M_{\pi^+\pi^-\pi^0}$ to extract the yields of $\omega\phi$ signal and non- ω/ϕ background in the control sample. In the 2-D fit, the ϕ signal in the $M_{K^+K^-}$ distribution is modeled using the signal MC shape convolved with a Gaussian function, while the continuum background is described by an inverse-ARGUS function [34]. The ω signal in the $M_{\pi^+\pi^-\pi^0}$ distribution is modeled using the signal MC shape convolved with a Gaussian function, and the continuum background is described with a second-order Chebyshev polynomial. In the fit, the signal MC sample is the process $J/\psi \rightarrow \gamma\omega\phi$ and with the similar PHSP variables $\vec{\xi}$ of data. The overall probability density function (p.d.f.) in the 2-D fit is the sum of four components, *i.e.* the ϕ and ω signal, the non- ϕ and ω background, the ϕ and non- ω background, as well as non- ϕ and non- ω background. Each component is the product of the corresponding functions for the $M_{K^+K^-}$ and $M_{\pi^+\pi^-\pi^0}$ distributions. With the above process, the Q-weights are obtained for the every individual candidate event with the signal yields from the above fit and the number of events of the control sample. From the fit, the Q-weights for each candidate event are obtained as the ratio of the signal yield to the number of events in the control sample. Using these Q-weights, the distributions for Q-weighted signal events and (1-Q)-weighted non- ω/ϕ background events are shown in Fig. 3.

The Q-weight method for estimating the non- ω/ϕ background has been thoroughly validated using MC samples in this analysis.

V. SIGNAL EXTRACTION

A. Fitting method

In Fig. 3, the $\eta_c \rightarrow \omega\phi$ signal is evident after adopting the Q-weight method. To extract the η_c signal yield, an unbinned maximum likelihood fit is performed on the $M_{K^+K^-\pi^+\pi^-\pi^0}$ distribution. In the fit, the line shape of the $\eta_c \rightarrow \omega\phi$ signal is modeled using the MC simulated sample generated by an M1 transition:

$$E_\gamma^3 \times BW(m) \times f_d(E_\gamma), \quad (2)$$

where E_γ is the energy of the radiative photon as described in Sec. II, and $BW(m)$ is the Breit-Wigner function of the η_c ,

$$BW(m) = \left| \frac{1}{m^2 - M_R^2 + iM_R\Gamma_R} \right|^2, \quad (3)$$

where $m = M_{K^+K^-\pi^+\pi^-\pi^0}$, and $f_d(E_\gamma)$ is a function that damps the diverging tail arising from the E_γ^3 dependence. In this analysis, the damping function $f_d(E_\gamma)$ [28] adopted from the CLEO collaboration [27] and is given by:

$$f_d(E_\gamma) = \exp(-E_\gamma^2/8\beta^2), \quad (4)$$

where the form factor parameter $\beta = 65.0 \pm 2.5$ MeV.

The non- ω/ϕ background is described by the p.d.f. extracted from the corresponding background curve in Fig. 3, with its amplitude fixed to the results obtained from the Q-weight method. The background from $J/\psi \rightarrow \gamma\omega\phi$ without the η_c signal is described by an ARGUS function [34], with its parameters left free in the fit. Previous studies indicate no significant structures in the distribution within the region of interest. Additionally, contributions from resonances peaking in the low-mass region are expected to be small, based on the results of amplitude analyses [35, 36]. Interference between the η_c signal and the continuum 0^{-+} contribution is not considered in the fit.

The fitting result is shown in Fig. 4. The obtained η_c signal yield is $N_{\text{obs}} = 118 \pm 28$, where the uncertainty is statistical only. An input-output check is performed to validate the reliability of the fitting procedure, and no significant bias is observed.

B. Numerical result

The branching fraction of $\eta_c \rightarrow \omega\phi$ is calculated using

$$\mathcal{B}(\eta_c \rightarrow \omega\phi) = \frac{N_{\text{obs}}}{N_{J/\psi} \cdot \mathcal{B}_{J/\psi} \cdot \mathcal{B}_\phi \cdot \mathcal{B}_\omega \cdot \mathcal{B}_{\pi^0} \cdot \epsilon}, \quad (5)$$

where $N_{J/\psi}$ is the total number of J/ψ events, and $\epsilon = 5.01\%$ is the signal detection efficiency. $\mathcal{B}_{J/\psi}$, \mathcal{B}_ϕ , \mathcal{B}_ω and

TABLE I. Definitions and normalization of coordinates in the multidimensional space.

Coordinate	Description	Δ_k
$\cos(\theta_\gamma)$	Polar angle of the radiative photon	2
$\cos(\theta_\omega)$	Polar angle of the ω	2
φ_ω	Azimuthal angle of the ω in η_c rest frame	2π
$\cos(\theta_\phi)$	Polar angle of the ϕ	2
φ_ϕ	Azimuthal angle of the ϕ in η_c rest frame	2π
$\cos(\theta_{K^+})$	Polar angle of the K^+	2
φ_{K^+}	Azimuthal angle of the K^+	2π
$m^2(\omega\phi)$	Invariant mass square of the $\omega\phi$ system	Standard deviation
$m^2(\gamma\omega)$	Invariant mass square of the $\gamma\omega$ system	Standard deviation
$m^2(\gamma\phi)$	Invariant mass square of the $\gamma\phi$ system	Standard deviation
$\lambda_\omega/\lambda_{\max}$	Normalized slope parameter of the ω Dalitz plot	1

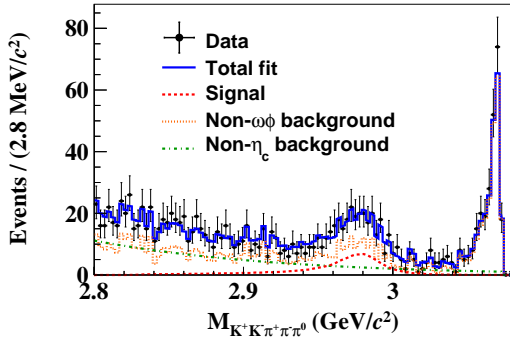


FIG. 4. The $M_{K^+K^-\pi^+\pi^-\pi^0}$ distribution of the accepted candidates for $\eta_c \rightarrow \omega\phi$. The black dots with error bars represent data and the blue curve represents the accumulated fit curve. The red dashed curve represents the signal, the orange dotted curve and green dash-dot curve represent the non- ω/ϕ background estimated by Q-weight method and the non- η_c background, respectively.

\mathcal{B}_{π^0} are the branching fractions of the decays $J/\psi \rightarrow \gamma\eta_c$, $\phi \rightarrow K^+K^-$, $\omega \rightarrow \pi^+\pi^-\pi^0$ and $\pi^0 \rightarrow \gamma\gamma$, respectively, cited from the PDG [2]. With these inputs, the branching fraction is determined to be $\mathcal{B}(\eta_c \rightarrow \omega\phi) = (3.86 \pm 0.92) \times 10^{-5}$, where the uncertainty is statistical only. This result is consistent with the corresponding upper limit of 2.5×10^{-4} at the 90% confidence level reported in the PDG.

VI. SYSTEMATIC UNCERTAINTIES

Several sources of systematic uncertainty are considered in the measurement of the branching fraction, including external input parameters, signal detection efficiency, and signal extraction.

The uncertainty of the total number of J/ψ events is 0.5% according to Ref. [13]. The uncertainties in the branching fractions of $J/\psi \rightarrow \gamma\eta_c$, $\omega \rightarrow \pi^+\pi^-\pi^0$, $\phi \rightarrow K^+K^-$ and $\pi^0 \rightarrow \gamma\gamma$, taken from the PDG [2], is 10.0%.

The tracking efficiencies for charged pions and kaons are studied with the control samples of $\psi' \rightarrow \pi^+\pi^-J/\psi \rightarrow \pi^+\pi^-l^+l^-$ and $J/\psi \rightarrow \rho^0\pi^0 \rightarrow$

$\pi^+\pi^-\pi^0$ [37], as well as $J/\psi \rightarrow K_S^0\bar{K}^{*0}(892) + c.c. \rightarrow K_S^0K^+\pi^- + c.c.$ [37], respectively. The efficiency difference between data and MC simulation is less than 1% per pion or kaon. Therefore, the total systematic uncertainty due to tracking for the four charged particles is assigned as 4.0% in total. The PID efficiencies for charged pions and kaons are estimated with control samples of $J/\psi \rightarrow \pi^+\pi^-\pi^0$ [37] and $J/\psi \rightarrow K^+K^-\pi^0$ [37], respectively. The efficiency difference between data and MC simulation is less than 1% per pion or kaon, leading to a total systematic uncertainty of 4.0% for PID. The photon detection efficiency is studied with the control sample of $J/\psi \rightarrow \rho^0\pi^0 \rightarrow \pi^+\pi^-\pi^0$ [38]. The difference in the efficiency between data and MC simulation, 1%, is taken as the uncertainty of per photon, resulting in a total systematic uncertainty of 3.0% for the three photons. The uncertainty in the kinematic fit arises primarily from inconsistencies in the kinematic variables of charged tracks. A helix parameter correction is applied to the signal MC sample to minimize data-MC differences [39]. The resulting change in detection efficiency, 6.0%, is considered as the systematic uncertainty. The uncertainties of ϕ and ω signal regions are due to resolution differences between data and MC simulation. Fits to the $M_{\pi^+\pi^-\pi^0}$ and $M_{K^+K^-}$ distributions of data are performed using the corresponding MC simulation shapes convolved with Gaussian functions. The resulting changes in detection efficiency, 0.5% for ω and 0.1% for ϕ , are assigned as systematic uncertainties.

The uncertainty of the π^0 decay angle requirement is studied with the control sample of $J/\psi \rightarrow \pi^+\pi^-\pi^0$. The efficiency difference between data and MC simulation, 1.0%, is taken as the systematic uncertainty. The uncertainty of the η' veto is studied using an alternative signal MC sample generated by varying the input form factor parameter β by $\pm 1\sigma$. The resulting efficiency difference, 0.1%, is taken as the systematic uncertainty.

The uncertainty of the η_c signal MC shape is studied with alternative signal MC samples. These include variations in the signal model parameters by $\pm 1\sigma$ and the use of a damping factor employed by the KEDR experiment [40, 41]. The alternative option of $f_d(E_\gamma)$ used by the KEDR experiment [40, 41]:

$$f_d(E_\gamma) = \frac{E_0^2}{E_0 E_\gamma + (E_\gamma - E_0)^2}, \quad (6)$$

where $E_0 = \frac{m_{J/\psi}^2 - m_c^2}{2m_{J/\psi}}$. The largest change in the measured branching fraction, 1.5%, is taken as the systematic uncertainty. The uncertainty due to the η_c width is studied by varying the world average η_c width within its uncertainty. The resulting largest change in the branching fraction, 3.0%, is assigned as the systematic uncertainty. The uncertainty of the shape of the $J/\psi \rightarrow \gamma\omega\phi$ non-peaking background is studied with an alternative fit performed by replacing the ARGUS function with a third-order Chebyshev polynomial. The resulting change in the signal yield, 2.5%, is taken as the corresponding uncertainty. The uncertainty of the Q-weight method is studied with MC sample. MC sample containing background and signal are generated and subjected to Q-weight method. The deviation between the number of generated signal events and the sum of obtained Q-weight is determined to be 7.6%, which is taken as the systematic uncertainty of the method. The uncertainty in the fit range is studied by performing alternative fits with different ranges: [2775.0, 3100.0] MeV/ c^2 and [2825.0, 3100.0] MeV/ c^2 . The largest change in the signal yield, 1.0%, is taken as the systematic uncertainty.

TABLE II. Sources and assigned systematic uncertainties in the branching fraction measurement.

Source	Uncertainty (%)
Total number of J/ψ events	0.5
Intermediate branching fractions	10.0
Tracking efficiency	4.0
PID	4.0
Photon detection	3.0
Kinematic fit	6.0
ω signal region	0.5
ϕ signal region	0.1
Decay angle of π^0	1.0
η' veto	0.1
Signal MC shape of η_c	1.5
η_c width	3.0
Non-peaking background description	2.5
Non- $\omega\phi$ background	7.6
Fit range	1.0
Total	16.0

All systematic uncertainties are summarized in Table II. The total systematic uncertainty is calculated as the square root of the quadratic sum of the individual contributions. The η_c signal significance is estimated from the change of likelihood and the change of number of degrees of freedom with and without the η_c signal included in the fit. The significance varies during systematic checks, and the minimum value, 4.0σ , is taken as the final signal significance.

VII. SUMMARY AND DISCUSSION

Using a sample of $(10087 \pm 44) \times 10^6$ J/ψ events [13] collected with the BESIII detector at BEPCII, we report the first evidence for the doubly OZI-suppressed decay $\eta_c \rightarrow \omega\phi$ with a significance of 4.0σ . This result is achieved after effectively suppressing the high and complex back-

grounds using the Q-weight method. Although potential interference effects are not considered in this analysis, they may have an impact on the measured branching fraction. The branching fraction of $\eta_c \rightarrow \omega\phi$ is determined to be $\mathcal{B}(\eta_c \rightarrow \omega\phi) = (3.86 \pm 0.92 \pm 0.62) \times 10^{-5}$, where the first uncertainty is statistical and the second is systematic. This result, together with the previously measured branching fractions of $\eta_c \rightarrow \omega\omega$ and $\eta_c \rightarrow \phi\phi$ [5, 6], provides robust inputs for studying the mechanisms of OZI-suppressed decays in J/ψ and η_c systems [11] [12]. Furthermore, this analysis offers important insights for establishing theoretical models based on the Helicity Selection Rule (HSR) and contributes to a deeper understanding of the $\eta_c \rightarrow VV$ process.

ACKNOWLEDGMENTS

The BESIII collaboration thanks the staff of BEPCII, the IHEP computing center and the supercomputing center of the University of Science and Technology of China (USTC) for their strong support. This work is supported in part by National Key R&D Program of China under Contracts Nos. 2020YFA0406300, 2020YFA0406400, 2023YFA1609400, 2023YFA1606000; National Natural Science Foundation of China (NSFC) under Contracts Nos. 11625523, 11635010, 11735014, 11935015, 11935016, 11935018, 12025502, 12035009, 12035013, 12061131003, 12105276, 12122509, 12192260, 12192261, 12192262, 12192263, 12192264, 12192265, 12221005, 12225509, 12235017, 12361141819; the Chinese Academy of Sciences (CAS) Large-Scale Scientific Facility Program; the CAS Center for Excellence in Particle Physics (CCEPP); Joint Large-Scale Scientific Facility Funds of the NSFC and CAS under Contracts Nos. U2032111, U1732263, U1832103, U1832207; CAS Youth Team Program under Contract No. YSBR-101; CAS under Contract No. YSBR-101; 100 Talents Program of CAS; The Institute of Nuclear and Particle Physics (IN-PAC) and Shanghai Key Laboratory for Particle Physics and Cosmology; Agencia Nacional de Investigación y Desarrollo de Chile (ANID), Chile under Contract No. ANID PIA/APOYO AFB230003; German Research Foundation DFG under Contract No. FOR5327; Istituto Nazionale di Fisica Nucleare, Italy; Knut and Alice Wallenberg Foundation under Contracts Nos. 2021.0174, 2021.0299; Ministry of Development of Turkey under Contract No. DPT2006K-120470; National Research Foundation of Korea under Contract No. NRF-2022R1A2C1092335; National Science and Technology fund of Mongolia; National Science Research and Innovation Fund (NSRF) via the Program Management Unit for Human Resources & Institutional Development, Research and Innovation of Thailand under Contract No. B50G670107; Polish National Science Centre under Contract No. 2019/35/O/ST2/02907; Swedish Research Council under Contract No. 2019.04595; The Swedish Foundation for International Cooperation in Research and Higher Education under Contract No. CH2018-7756; U. S. Department of Energy under Contract No. DE-FG02-05ER41374

-
- [1] R. Partridge *et al.*, *Phys. Rev. Lett.* **45**, 1150 (1980).
- [2] S. Navas *et al.* (Particle Data Group), *Phys. Rev. D* **110**, 030001 (2024).
- [3] S. Okubo, *Phys. Lett.* **5**, 165 (1963).
- [4] S. J. Brodsky and G. P. Lepage, *Phys. Rev. D* **24**, 2848 (1981).
- [5] M. Ablikim *et al.* (BESIII Collaboration), *Phys. Rev. D* **100**, 052012 (2019).
- [6] M. Ablikim *et al.* (BESIII Collaboration), *Phys. Rev. D* **95**, 092004 (2017).
- [7] Z. Q. Liu *et al.* (Belle Collaboration), *Phys. Rev. Lett.* **108**, 232001 (2012).
- [8] P. Sun, G. Hao, and C. F. Qiao, *Phys. Lett. B* **702**, 49 (2011).
- [9] Q. Zhao, *Phys. Lett. B* **636**, 197 (2006).
- [10] T. Feldmann and P. Kroll, *Phys. Rev. D* **62**, 074006 (2000).
- [11] A. Seiden, H. F. W. Sadrozinski, and H. E. Haber, *Phys. Rev. D* **38**, 824 (1988).
- [12] H. E. Haber and J. Perrier, *Phys. Rev. D* **32**, 2961 (1985).
- [13] M. Ablikim *et al.* (BESIII Collaboration), *Chin. Phys. C* **46**, 074001 (2022).
- [14] M. Ablikim *et al.* (BESIII Collaboration), *Nucl. Instrum. Meth. A* **614**, 345 (2010).
- [15] C. Yu *et al.*, in *7th International Particle Accelerator Conference* (2016) p. TUYA01.
- [16] M. Ablikim *et al.* (BESIII Collaboration), *Chin. Phys. C* **44**, 040001 (2020).
- [17] X. Li *et al.*, *Radiat. Detect. Technol. Methods* **1**, 13 (2017).
- [18] Y.-X. Guo *et al.*, *Radiat. Detect. Technol. Methods* **1**, 15 (2017).
- [19] P. Cao *et al.*, *Nucl. Instrum. Meth. A* **953**, 163053 (2020).
- [20] S. Agostinelli *et al.* (GEANT4 Collaboration), *Nucl. Instrum. Meth. A* **506**, 250 (2003).
- [21] S. Jadach, B. F. L. Ward, and Z. Was, *Comput. Phys. Commun.* **130**, 260 (2000).
- [22] D. J. Lange, *Nucl. Instrum. Meth. A* **462**, 152 (2001).
- [23] R. G. Ping, *Chin. Phys. C* **32**, 599 (2008).
- [24] J. C. Chen, G. S. Huang, X. R. Qi, D. H. Zhang, and Y. S. Zhu, *Phys. Rev. D* **62**, 034003 (2000).
- [25] R. L. Yang, R. G. Ping, and H. Chen, *Chin. Phys. Lett.* **31**, 061301 (2014).
- [26] E. Barberio, B. van Eijk, and Z. Was, *Computer. Phys. Commun.* **66**, 115 (1991).
- [27] R. E. Mitchell *et al.* (CLEO Collaboration), *Phys. Rev. Lett.* **106**, 159903 (2011).
- [28] N. Brambilla, Y. Jia, and A. Vairo, *Phys. Rev. D* **73**, 054005 (2006).
- [29] M. Ablikim *et al.* (BESIII Collaboration), *Phys. Rev. D* **98**, 112007 (2018).
- [30] X. Zhou, S. Du, G. Li, and C. Shen, *Computer. Phys. Commun.* **258**, 107540 (2021).
- [31] M. Williams, M. Bellis, and C. A. Meyer, *JINST* **4**, P10003 (2009).
- [32] M. Williams *et al.* (CLAS Collaboration), *Phys. Rev. C* **80**, 065208 (2009).
- [33] C. Amsler *et al.*, *Eur. Phys. J. C* **75**, 124 (2015).
- [34] H. Albrecht *et al.* (ARGUS Collaboration), *Phys. Lett. B* **241**, 278 (1990).
- [35] M. Ablikim *et al.* (BESIII Collaboration), *Phys. Rev. Lett.* **96**, 162002 (2006).
- [36] M. Ablikim *et al.* (BESIII Collaboration), *Phys. Rev. D* **87**, 032008 (2013).
- [37] M. Ablikim *et al.* (BESIII Collaboration), *Phys. Rev. D* **83**, 112005 (2011).
- [38] M. Ablikim *et al.* (BESIII Collaboration), *Phys. Rev. D* **81**, 052005 (2010).
- [39] M. Ablikim *et al.* (BESIII Collaboration), *Phys. Rev. D* **87**, 012002 (2013).
- [40] V. Anashin *et al.*, *Int. J. Mod. Phys. Conf. Ser.* **02**, 188 (2011).
- [41] V. Anashin *et al.*, *Phys. Lett. B* **738**, 391 (2014).